

# Capacity of Finite-State Channels with Delayed Feedback

Bashar Huleihel      Oron Sabag      Haim H. Permuter      Victoria Kostina  
Ben-Gurion University    Hebrew University of Jerusalem    Ben-Gurion University      Caltech  
basharh@post.bgu.ac.il      oron.sabag@mail.huji.ac.il      haimp@bgu.ac.il      vkostina@caltech.edu

## Abstract

In this paper, we investigate the capacity of finite-state channels (FSCs) in presence of delayed feedback. We show that the capacity of a FSC with delayed feedback can be computed as that of a new FSC with instantaneous feedback and an extended state. Consequently, graph-based methods to obtain computable upper and lower bounds on the delayed feedback capacity of unifilar FSCs are proposed. Based on these methods, we establish that the capacity of the trapdoor channel with delayed feedback of two time instances is given by  $\log_2\left(\frac{3}{2}\right)$ . In addition, we derive an analytical upper bound on the delayed feedback capacity of the binary symmetric channel with a no consecutive ones input constraint. This bound also serves as a novel upper bound on its non-feedback capacity, which outperforms all previously known bounds. Lastly, we demonstrate that feedback does improve the capacity of the dicode erasure channel.

## I. INTRODUCTION

A finite-state channel (FSC) is a widely used statistical model for a channel with memory [2]–[4]. The memory of this channel is represented by an underlying channel state that takes values from a finite set. This model has been used in many practical applications, including wireless communication [5]–[7], molecular communication [8], [9], and magnetic recording [10]. An example of its versatility is the ability to model a memoryless channel with an input constraint by introducing a finite-state machine that tracks the forbidden constraint, and a sink state whose capacity is zero and is reached when the constraint is violated. Generally speaking, the capacity formula of a FSC, whether or not feedback is allowed, is given by a multi-letter expression which is hard to evaluate. The main focus of this paper is on an important class of FSCs, known as unifilar FSCs. For these channels, the new channel state is determined by a time-invariant function of the previous channel state, the current channel input, and the current channel output.

The capacity of a unifilar FSC with instantaneous feedback has been broadly investigated in the literature, while instantaneous feedback refers to the case where at time  $t$ , the encoder has access to the channel outputs up to time  $t - 1$ . This has resulted in several powerful methodologies that have been employed to derive simple capacity expressions and optimal coding schemes for well-known instances of unifilar FSCs with feedback [11]–[20]. We mention here three essential works that will be utilized in the current paper: in [21], [22], for a given  $Q$ -graph<sup>1</sup>, single-letter upper and lower bounds on the feedback capacity of unifilar FSCs were introduced, as well as a methodology to evaluate the bounds; in [23], an alternative methodology to derive computable capacity upper bounds was proposed. In particular, in [23] it was shown that the dual capacity upper bound can be formulated as a simple Markov decision process (MDP) with the MDP states, actions, and disturbances taking values within finite sets. The main advantage of the duality-based upper bound compared to the single-letter  $Q$ -graph upper bound is the simplicity of deriving analytical upper bounds. However, the duality-based bounds require the specification of a  $Q$ -graph and a corresponding test distribution, while in the case of the  $Q$ -graph single-letter bounds, only

This paper was presented in part at the 2022 IEEE International Symposium on Information Theory [1].

<sup>1</sup>The  $Q$ -graph is an auxiliary directed graph that is used to map channel output sequences onto one of the graph nodes (e.g. see Fig. 4).

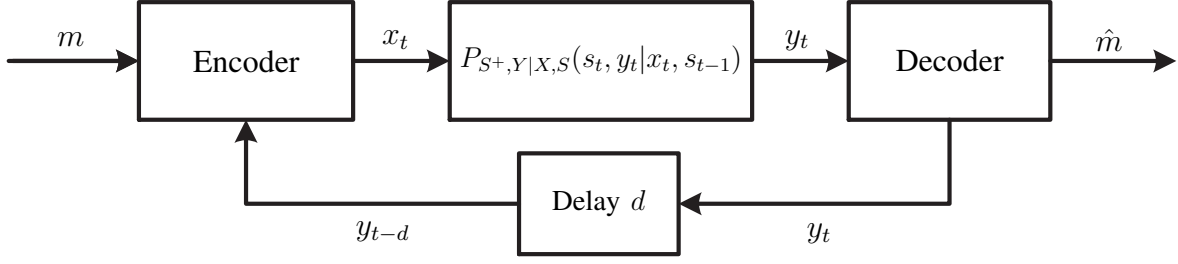


Fig. 1. Finite-state channel with delayed feedback of  $d$  time instances.

the  $Q$ -graph itself needs to be determined. Finding the optimal auxiliary parameters for the test distribution to yield tight bounds can be a challenging task. Nevertheless, in our current work, we are able to identify both the  $Q$ -graph and its test distribution so that the duality technique is utilized to derive analytical upper bounds.

In this paper, we investigate the delayed feedback capacity of FSCs. This means that, in the case of a delay of  $d$  time instances, the encoder has access to the channel outputs up to time  $t - d$ , in contrast to the standard feedback definition of access up to time  $t - 1$  (see Fig. 1). Our objective is two-fold: first, to investigate the capacity of FSCs in various feedback scenarios; and second, to derive upper bounds on the feedforward capacity (i.e., the capacity without feedback), as it is a known fact that feedback can only increase the feedforward capacity. While studying the delayed feedback capacity is important task on its own, it also helps us achieve our second objective.

#### A. Main Contributions

Our first contribution is to show that a unifilar FSC with delayed feedback can be transformed into a unifilar FSC with instantaneous feedback to which the methodologies from [21]–[23] apply:

- We show that the capacity of a general FSC with delayed feedback can be computed as the capacity of a transformed FSC with instantaneous feedback. We define the new channel state as  $\tilde{S}_{t-1} = (S_{t-d}, X_{t-d+1}^{t-1})$ , the new channel output as  $\tilde{Y}_t = Y_{t-d+1}$ , and leave the channel input unchanged, i.e.,  $\tilde{X}_t = X_t$ . We prove that this new channel is an FSC and that its capacity with instantaneous feedback is equal to the capacity of the original FSC with delayed feedback of  $d$  time instances.
- We demonstrate that if the original channel is a unifilar FSC, then the transformed FSC is a unifilar FSC as well.

We investigate the delayed feedback capacity of several important FSCs, and provide novel results on both their delayed feedback capacity and feedforward capacity:

- Despite the extensive research efforts [12], [24]–[28] dedicated to the trapdoor channel [29], see Fig. 2, its feedforward capacity has remained an open problem for over sixty years. In [12], it was shown that the feedback capacity of the trapdoor channel is equal to  $C_1^{\text{fb}} = \log_2 \left( \frac{1+\sqrt{5}}{2} \right) \approx 0.6942$ . In this paper, we consider the trapdoor channel with delayed feedback of  $d = 2$  time instances, and show that the capacity in this scenario is equal to  $C_2^{\text{fb}} = \log_2 \left( \frac{3}{2} \right) \approx 0.5850$ . Compared to the feedback capacity, this value is much closer to the lower bound on the feedforward capacity of 0.572 [26]. Further, by investigating a greater delay of the feedback, we provide a new upper bound on its feedforward capacity, which is approximately equal to 0.5765.
- We study the capacity of the binary symmetric channel (BSC) in the case where the input sequence is not allowed to contain two consecutive ones. The feedforward capacity in this scenario is still unknown [19], [30]–[33]. We derive an analytical upper bound on its capacity with delayed feedback of 2 time instances that also serves as a novel upper bound on the feedforward capacity.

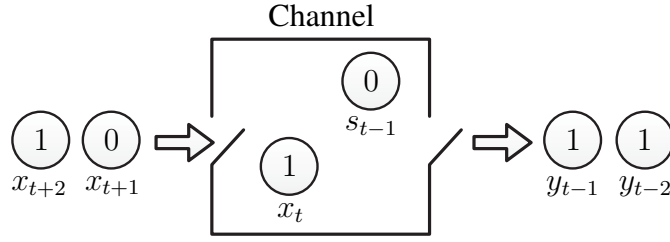


Fig. 2. The trapdoor channel. The channel can be viewed as a box in which at time  $t$  a labelled ball  $s_{t-1}$  (channel state) lies. Then, a new ball  $x_t$  (channel input) is inserted into the box, and the channel output  $y_t$  is chosen with equal probability as either  $s_{t-1}$  or  $x_t$ . The remaining ball in the box (either  $s_{t-1}$  or  $x_t$ ) is now called  $s_t$  and serves as the channel state for the next time-instance.

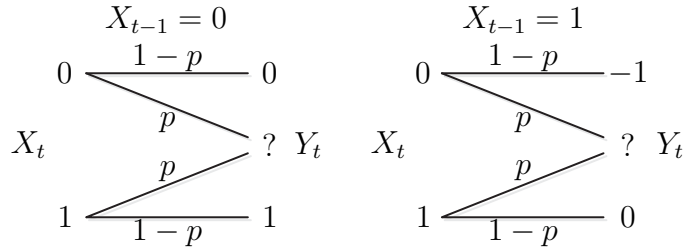


Fig. 3. The DEC. The inputs take values from the binary alphabet while the outputs take values in  $\mathcal{Y} = \{-1, 0, 1, ?\}$ . Given an input  $x_t$ , the output of the DEC is  $y_t = x_t - x_{t-1}$  with probability  $1 - p$ , or  $y_t = ?$  with probability  $p$ , where  $p \in [0, 1]$  is the channel parameter. The channel state is the previous input, i.e.  $s_{t-1} = x_{t-1}$ .

- We demonstrate that the feedback capacity of the dicode erasure channel (DEC) [34], [35], see Fig. 3, is not equal to its feedforward capacity, by providing a new upper bound on its feedforward capacity that lies slightly below the feedback capacity.

## B. Organization

The remainder of this paper is organized as follows. Section II introduces the notation and the model definition. Section III introduces computable upper and lower bounds on the capacity of unifilar FSCs with instantaneous feedback. Section IV presents our demonstration of the fact that the delayed feedback capacity problem can be reduced into an instantaneous feedback capacity problem, by appropriately reformulating the channel. Subsequently, we also introduce computable upper and lower bounds on the delayed feedback capacity of unifilar FSCs. Section V presents our main results regarding the capacity of the trapdoor channel. Section VI provides novel results concerning the feedforward capacities of the input-constrained BSC and the DEC, by investigating their delayed feedback capacity. Finally, our conclusions appear in Section VII. To preserve the flow of the presentation, some of the proofs are given in the appendices.

## II. NOTATION AND PRELIMINARIES

In this section, we introduce the notation, the model definition, and our MDP framework.

### A. Notation

Throughout this paper, random variables will be denoted by capital letters and their realizations will be denoted by lower-case letters, e.g.  $X$  and  $x$ , respectively. Calligraphic letters denote sets, e.g.  $\mathcal{X}$ . We use the notation  $X^n$  to denote the random vector  $(X_1, X_2, \dots, X_n)$  and  $x^n$  to denote the realization of such a random vector. The probability  $\Pr[X = x]$  is denoted by  $P_X(x)$ . When the random variable is clear from

the context, we write it in shorthand as  $P(x)$ . For a real number  $\alpha \in [0, 1]$ , we define  $\bar{\alpha} = 1 - \alpha$ . We use the convention that  $0 \log 0 = 0$ .

The directed information between  $X^n$  and  $Y^n$  is defined as

$$I(X^n \rightarrow Y^n) = \sum_{i=1}^n I(X^i; Y_i | Y^{i-1}).$$

The probability mass function of  $X^n$  *causally conditioned* on  $Y^{n-d}$  is defined as

$$P(x^n \| y^{n-d}) = \prod_{i=1}^n P(x_i | x^{i-1}, y^{i-d}).$$

We denote by  $C$ ,  $C_1^{\text{fb}}$ , and  $C_d^{\text{fb}}$ , the feedforward capacity (i.e. no feedback), the feedback capacity (the capacity with instantaneous feedback, i.e.  $d = 1$  in Fig. 1), and the  $d$  time instances delayed feedback capacity, respectively.

### B. Finite-state Channels

A FSC is defined statistically by a time-invariant transition probability kernel,  $P_{S^+, Y | X, S}$ , where  $X$ ,  $Y$ ,  $S$ ,  $S^+$  denote the channel input, output, and state before and after one transmission, respectively. The cardinalities  $\mathcal{X}, \mathcal{Y}, \mathcal{S}$  are assumed to be finite. Formally, given a message  $m$ , the channel has the following property:

$$P(s_t, y_t | x^t, y^{t-1}, s^{t-1}, m) = P_{S^+, Y | X, S}(s_t, y_t | x_t, s_{t-1}). \quad (1)$$

A unifilar FSC has the additional property that the state evolution is given by a time-invariant function,  $f(\cdot)$ , such that  $s_t = f(s_{t-1}, x_t, y_t)$ .

As shown in the theorem below, the feedback capacity of a strongly connected<sup>2</sup> FSC is given by a multi-letter expression that cannot be computed directly.

**Theorem 1** ([12], Th. 3). *The feedback capacity of a strongly connected FSC is*

$$C_1^{\text{fb}} = \lim_{n \rightarrow \infty} \frac{1}{n} \max_{P(x^n \| y^{n-1})} I(X^n \rightarrow Y^n). \quad (2)$$

In this paper, we consider a communication setting with delayed feedback as depicted in Fig. 1. The encoder has access to the message  $M$  and the channel outputs delayed by  $d$  time instances. That is, the encoder outputs  $x_t$  as a function of  $M$  and the channel outputs up to time  $t - d$ , where  $d \geq 1$  is a finite integer. This setting captures the conventional instantaneous feedback case when  $d = 1$ . An interesting problem beyond the scope of the current paper is to consider a delay parameter  $d$  that can scale with the block length communication. The channel input  $x_t$  then goes through a FSC, and the resulting output  $y_t$  enters the decoder. The encoder then receives the feedback sample with a delay of  $d$  time instances. When the feedback has a delay of  $d$  time instances, the maximization over the directed information in Theorem 1 is performed over  $P(x^n \| y^{n-d})$  instead of over  $P(x^n \| y^{n-1})$  [36].

<sup>2</sup>A FSC is strongly connected if for any states  $s, s' \in \mathcal{S}$ , there exist an integer  $T$  and an input distribution  $\{P_{X_t | S_{t-1}}\}_{t=1}^T$  such that  $\sum_{t=1}^T P_{S_t | S_0}(s | s') > 0$ .

### C. MDP Framework

MDP provide a mathematical framework for modeling decision-making problems in which the outcomes of actions are uncertain and dependent on the current state of the system. We consider an MDP problem with a state space  $\mathcal{Z}$ , an action space  $\mathcal{U}$ , and a disturbance space  $\mathcal{W}$ . The initial state  $z_0 \in \mathcal{Z}$  is randomly drawn from a distribution  $P_Z$ . At each time step  $t$ , the system is in a state  $z_{t-1} \in \mathcal{Z}$ , the decision-maker selects an action  $u_t \in \mathcal{U}$ , and a disturbance  $w_t \in \mathcal{W}$  is drawn according to a conditional distribution  $P_w(\cdot|z_{t-1}, u_t)$ . The state  $z_t$  then evolves according to a transition function  $F : \mathcal{Z} \times \mathcal{U} \times \mathcal{W} \rightarrow \mathcal{Z}$ , i.e.,  $z_t = F(z_{t-1}, u_t, w_t)$ .

The decision-maker selects the action  $u_t$  according to a function  $\mu_t$ , which maps histories  $h_t = (z_0, w_0, \dots, w_{t-1})$  onto actions, i.e.  $u_t = \mu_t(h_t)$ . Given a policy  $\pi = \{\mu_1, \mu_2, \dots\}$  and a bounded reward function  $g : \mathcal{Z} \times \mathcal{U} \rightarrow \mathbb{R}$ , the goal is to maximize the average reward over an infinite time horizon. The average reward achieved by policy  $\pi$  is defined as

$$\rho_\pi = \liminf_{n \rightarrow \infty} \frac{1}{n} \mathbb{E}_\pi \left[ \sum_{t=0}^{n-1} g(Z_t, \mu_{t+1}(h_{t+1})) \right].$$

The optimal average reward is denoted by  $\rho^*$  and is achieved by the policy that maximizes the expected sum of rewards over time, i.e.,  $\rho^* = \sup_\pi \rho_\pi$ .

The following theorem presents the Bellman equation in the context of the formulation defined above. The Bellman equation provides a sufficient condition for determining whether a given average reward is optimal.

**Theorem 2** (Bellman equation, [37]). *If a scalar  $\rho \in \mathbb{R}$  and a bounded function  $h : \mathcal{Z} \rightarrow \mathbb{R}$  satisfy*

$$\rho + h(z) = \sup_{u \in \mathcal{U}} \left( g(z, u) + \int P_w(dw|z, u) h(F(z, u, w)) \right), \quad \forall z \in \mathcal{Z}$$

*then  $\rho = \rho^*$ .*

## III. BOUNDS ON FEEDBACK CAPACITY

In this section we introduce computable bounds on the feedback capacity of unifilar FSCs. These bounds were introduced for unifilar FSCs with instantaneous feedback in [21], [23]. In Section IV, we demonstrate that they can be extended to the case of delayed feedback as well.

### A. The $Q$ -graph Bounds

We begin by introducing an auxiliary tool known as the  $Q$ -graph. For a fixed  $Q$ -graph, we then present the single-letter upper and lower bounds that were established in [21]. The  $Q$ -graph is a directed, connected, and labeled graph, for which each of its nodes have  $|\mathcal{Y}|$  outgoing edges with distinct labels from the channel output alphabet. Given an initial node, an output sequence,  $y^t$ , is mapped onto a unique node by walking along the labeled edges. An example of a  $Q$ -graph is provided in Fig. 4. The induced mapping is denoted by  $\Phi_t : \mathcal{Y}^t \rightarrow \mathcal{Q}$ , which can be presented alternatively as a function  $\phi : \mathcal{Q} \times \mathcal{Y} \rightarrow \mathcal{Q}$ . Namely, a new graph node can be computed as a time-invariant function of the previous node and a channel output.

**Remark 1.** A special case of a  $Q$ -graph is a  $k$ th-order Markov  $Q$ -graph, which is defined on the set of nodes  $\mathcal{Q} = \mathcal{Y}^k$ ; for each node  $q = (y_1, y_2, \dots, y_k)$ , the outgoing edge labeled  $y \in \mathcal{Y}$  goes to the node  $(y_2, \dots, y_k, y)$ . For instance, Fig. 4 shows a Markov  $Q$ -graph with  $\mathcal{Y} = \{0, 1\}$  and  $k = 1$ .

For a fixed FSC and a given  $Q$ -graph, we construct the  $(S, Q)$ -graph, an additional directed graph that combines both the information on the  $Q$ -graph and the evolution of the channel states. Specifically, split each node in the  $Q$ -graph into  $|\mathcal{S}|$  new nodes, which are represented by pairs  $(s, q) \in \mathcal{S} \times \mathcal{Q}$ . Then, an edge labeled  $(x, y)$  from node  $(s, q)$  to node  $(s^+, q^+)$  exists if and only if there is a pair  $(x, y)$  such

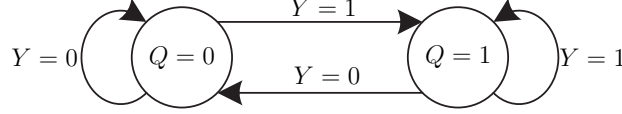


Fig. 4. An example of a  $Q$ -graph with  $\mathcal{Q} = 2$  and  $\mathcal{Y} = \{0, 1\}$ .

that  $s^+ = f(s, x, y)$ ,  $q^+ = \phi(q, y)$ , and  $P(y|x, s) > 0$ . The pair of functions  $(f, \phi)$  are given by the channel state transition and the fixed  $Q$ -graph. For any choice of input distribution  $P_{X|S, Q}$ , the transition probabilities on the edges of the  $(S, Q)$ -graph are computed as

$$\begin{aligned} P(s^+, q^+|s, q) &= \sum_{x, y} P(x, y, s^+, q^+|s, q) \\ &\stackrel{(a)}{=} \sum_{x, y} P(x|s, q) P(y|x, s) \mathbb{1}\{q^+ = \phi(q, y)\} \mathbb{1}\{s^+ = f(s, x, y)\}, \end{aligned} \quad (3)$$

where (a) follows by the channel law and by the fact that  $q^+$  is a deterministic function of  $(q, y)$ . We define the notation  $\mathcal{P}_\pi$  as the set of input distributions  $P_{X|S, Q}$  that induce a unique stationary distribution on  $(S, Q)$ , namely, their corresponding  $(S, Q)$ -graph is irreducible and aperiodic.

In the following theorem we introduce the upper bound.

**Theorem 3.** [21, Theorem 2] *The feedback capacity of a strongly connected unifilar FSC, where the initial state is available to both the encoder and the decoder, is bounded by*

$$C_1^{\text{fb}} \leq \sup_{P_{X|S, Q} \in \mathcal{P}_\pi} I(X, S; Y|Q), \quad (4)$$

for all  $Q$ -graphs for which the  $(S, Q)$ -graph has a single and aperiodic closed communicating class. The joint distribution is  $P_{Y, X, S, Q} = P_{Y|X, S} P_{X|S, Q} \pi_{S, Q}$ , where  $\pi_{S, Q}$  is the stationary distribution of the  $(S, Q)$ -graph.

We proceed to describe the lower bound. Let us first define a property called the *BCJR-invariant input*. An input distribution  $P_{X|S, Q}$  is said to be an *aperiodic input* if its  $(S, Q)$ -graph is aperiodic, and an aperiodic input distribution is said to be *BCJR-invariant* if the Markov chain  $S^+ - Q^+ - (Q, Y)$  holds. A simple verification of the Markov chain is given by the following equation:

$$\pi(s^+|q^+) = \frac{\sum_{x, s} \pi(s|q) P(x|s, q) P(y|x, s) \mathbb{1}_{\{s^+ = f(x, y, s)\}}}{\sum_{x', s'} \pi(s'|q) P(x'|s', q) P(y|x', s')}, \quad (5)$$

which needs to hold for all  $(s^+, q, y)$  and  $q^+ = \phi(q, y)$ .

Now that we have defined a BCJR-invariant input distribution, the lower bound can be introduced.

**Theorem 4.** [21, Theorem 3] *If the initial state  $s_0$  is available to both the encoder and the decoder, then the feedback capacity of a strongly connected unifilar FSC is bounded by*

$$C_1^{\text{fb}} \geq I(X, S; Y|Q), \quad (6)$$

for all aperiodic inputs  $P_{X|S, Q} \in \mathcal{P}_\pi$  that are BCJR-invariant, and for all irreducible  $Q$ -graphs with  $q_0$  such that  $(s_0, q_0)$  lies in an aperiodic closed communicating class.

Henceforth, we refer to a pair of a  $Q$ -graph and an input distribution  $P_{X|S, Q}$  that satisfies the BCJR-invariant property as a *graph-based encoder*.

**Remark 2.** The upper bound in Theorem 3 can be formulated as a convex optimization [22]. As a result, for a fixed  $Q$ -graph, the upper bound can be efficiently evaluated. On the other hand, the lower bound optimization results in a non-convex optimization problem, but it still has the advantage that any feasible point (i.e. BCJR-invariant input distribution) induces a graph-based encoder. It was shown in [22] that any graph-based encoder implies a simple coding scheme that achieves the lower bound. The scheme is based on an extension of posterior matching [38] to channels with memory [19], [22].

**Remark 3.** The selection of the  $Q$ -graph significantly impacts the performance of the bounds. To identify a  $Q$ -graph that will result in capacity-achieving bounds, we suggest conducting an exhaustive search over all possible  $Q$ -graphs, as explained in detail in [22]. While such an exploration can become computationally expensive with increasing  $Q$ -graph size, it is often sufficient to consider a small cardinality graph to obtain tight or nearly tight bounds. Another approach is to evaluate the performance of Markov  $Q$ -graphs, which often provide good bounds. A Matlab implementation of the optimization problems, including the  $Q$ -graph search methods, is available in [39].

### B. Upper Bounds via Duality

Here we present computable upper bounds on the capacity of unifilar FSCs from [23], that are based on the dual capacity upper bound [40]. For the sake of clarity, we first introduce the dual capacity upper bound for a discrete memoryless channel. Specifically, for a memoryless channel,  $P_{Y|X}$ , and for any choice of a test distribution,  $T_Y$ , on the channel output alphabet, the dual capacity upper bound states that

$$C \leq \max_{x \in \mathcal{X}} D(P_{Y|X=x} \| T_Y). \quad (7)$$

The choice of the test distribution is crucial since it directly affects the performance of the bound. If the test distribution is equal to the optimal output distribution, then the upper bound is tight. For FSCs, the dual upper bound depends on a test distribution,  $T_{Y^n}$ , with memory. In [23], [28], test distributions that are structured on a  $Q$ -graph were proposed, that is, the following equality holds:

$$T_{Y^n}(y^n) = \prod_{t=1}^n T_{Y|Q}(y_t | q_{t-1}), \quad (8)$$

where  $q_{t-1} = \Phi(y^{t-1})$ . We refer to such test distributions as *graph-based test distributions*. The use of graph-based test distributions yielded the result in the theorem below.

**Theorem 5** (Computable upper bounds). [23, Theorem 4] *For any graph-based test distribution  $T_{Y|Q}$ , the feedback capacity of a strongly connected unifilar FSC is bounded by*

$$C_1^{\text{fb}} \leq \lim_{n \rightarrow \infty} \max_{f(x^n \| y^{n-1})} \min_{s_0, q_0} \frac{1}{n} \sum_{i=1}^n \mathbb{E} \left[ D \left( P_{Y|X,S}(\cdot | x_i, S_{i-1}) \parallel T_{Y|Q}(\cdot | Q_{i-1}) \right) \right], \quad (9)$$

where  $f(x^n \| y^{n-1})$  stands for causal conditioning of deterministic functions, i.e.

$$f(x^n \| y^{n-1}) = \prod_i \mathbb{1}\{x_i = f_i(x^{i-1}, y^{i-1})\}.$$

Additionally, the upper bound in (9) defines an infinite-horizon average reward MDP that is presented in Table I.

The following theorem is a simplification of the Bellman equation in Theorem 2 for the case of the MDP formulation in Table I.

TABLE I  
MDP FORMULATION

MDP notations	Upper bound on capacity
MDP state	$z_{t-1} \triangleq (s_{t-1}, q_{t-1})$
Action	$u_t \triangleq x_t$
Disturbance	$w_t \triangleq y_t$
The reward	$g(z_{t-1}, u_t) \triangleq D(P_{Y X,S}(\cdot x_t, s_{t-1})    T_{Y Q}(\cdot q_{t-1}))$

**Theorem 6** (Bellman equation). *If there exists a scalar  $\rho \in \mathbb{R}$  and a bounded function  $h : \mathcal{S} \times \mathcal{Q} \rightarrow \mathbb{R}$  such that*

$$\rho + h(s, q) = \max_{x \in \mathcal{X}} \left( D(P_{Y|X,S}(\cdot|x, s) || T_{Y|Q}(\cdot|q)) + \sum_{y \in \mathcal{Y}} P(y|x, s) h(f(s, x, y), \phi(q, y)) \right), \quad (10)$$

*for all  $(s, q)$ , then  $\rho = \rho^*$ .*

Following Theorem 6, it is sufficient to solve the Bellman equation associated with the MDP problem in Table I to show that the feedback capacity of a given FSC is upper bounded by the induced average reward of the MDP.

**Remark 4.** The  $Q$ -graph upper bound, presented in Section III-A, provides an efficient approach for evaluating numerical upper bounds since it relies on a convex optimization problem [28]. However, obtaining analytical bounds using this methodology may be tedious as the KKT conditions need to be verified to derive the bounds. Therefore, to obtain analytical bounds (not just numerical ones), we prefer using the duality-based technique presented in this section. In particular, note that the MDP formulation in Table I consists of finite MDP states, actions, and disturbances. Thus, given an optimal policy, we only need to solve a finite set of linear equations to derive a conjectured solution for  $(\rho^*, h(\cdot))$ .

#### IV. COMPUTABLE BOUNDS ON DELAYED FEEDBACK CAPACITY

In this section we start with a general result, in which the delayed feedback capacity of any FSC can be computed as the instantaneous feedback capacity of a transformed FSC. By utilizing this reduction, we derive computable upper and lower bounds on the delayed feedback capacity of unifilar FSCs that are a straightforward extension of the  $Q$ -graph bounds from Section III-A. These new bounds are introduced in Section IV-B.

##### A. Delayed Feedback Capacity as Instantaneous Feedback Capacity

For a finite integer  $d \geq 1$  and for any FSC given by a transition kernel  $P_{Y,S+|X,S}$ , we define the following transformation:

- The channel state is  $\tilde{S}_t \triangleq (S_{t-d+1}, X_{t-d+2}^t)$ .
- The channel output is  $\tilde{Y}_t \triangleq Y_{t-d+1}$ .
- The channel input remains the same, i.e.  $\tilde{X}_t \triangleq X_t$ .

First, we will show that the above transformation defines a new FSC with a transition kernel  $P_{\tilde{Y}, \tilde{S}+|\tilde{X}, \tilde{S}}^d$ , where the superscript  $d$  emphasizes the transformation dependence on the delay  $d$ . That is, the new channel follows the time-invariant Markov property of FSCs in (1). Second, we show in the following theorem the relation between the channel capacity of the original FSC and its transformation.



**Theorem 7.** *The capacity of a FSC  $P_{Y,S+|X,S}$  with delayed feedback of  $d$  time instances is equal to the instantaneous feedback capacity of the FSC  $P_{\tilde{Y},\tilde{S}+|\tilde{X},\tilde{S}}^d$ . Furthermore, if the original FSC is unifilar, then the new transformed FSC is unifilar as well.*

It is important to note that the cardinality of the new channel state is  $|\tilde{\mathcal{S}}| = |\mathcal{S}| \cdot |\mathcal{X}|^{d-1}$ , while the cardinality of the channel state in the original channel is  $|\mathcal{S}|$ . That is, we pay the price of having a larger channel state space as a result of the delay.

*Proof of Theorem 7.* Given a FSC,  $P_{Y,S+|X,S}$ , define the new channel state as  $\tilde{S}_{t-1} = (S_{t-d}, X_{t-d+1}^{t-1})$ , let the channel output be  $\tilde{Y}_t = Y_{t-d+1}$ , and let the channel input remain the same, i.e.  $\tilde{X}_t = X_t$ . In the following, we show that the new channel is a FSC such that its capacity with instantaneous feedback is equal to the capacity of the original channel with delayed feedback of  $d$  time instances.

- Conditioned on the previous channel state  $\tilde{S}_{t-1}$ , the channel input  $\tilde{X}_t$ , and the channel output  $\tilde{Y}_t$ , the new channel state  $\tilde{S}_t$  is independent of any other previous states, inputs, and outputs. That is,

$$P(\tilde{s}_t | \tilde{x}^t, \tilde{y}^t, \tilde{s}^{t-1}) = P(\tilde{s}_t | \tilde{s}_{t-1}, \tilde{x}_t, \tilde{y}_t). \quad (11)$$

This equation holds due to the Markov chain  $(S_{t-d+1}, X_{t-d+2}^t) - (S_{t-d}, X_{t-d+1}^t, Y_{t-d+1}) - (X^{t-d}, Y^{t-d})$ , which follows directly by the Markov chain property of the original channel. In particular, since  $\tilde{S}_t = (S_{t-d+1}, X_{t-d+2}^t)$ , and since  $(\tilde{S}_{t-1}, \tilde{X}_t, \tilde{Y}_t)$  include  $(S_{t-d}, X_{t-d+1}^t, Y_{t-d+1})$ , (11) holds.

In addition, we show below that, if the original channel is a unifilar FSC, then the unifilar property also holds for the new induced channel. That is, we show that the new channel state  $\tilde{s}_t$  is a time-invariant function of  $\tilde{s}_{t-1}$ ,  $\tilde{x}_t$ , and  $\tilde{y}_t$ :

$$\begin{aligned} \tilde{s}_t &= (s_{t-d+1}, x_{t-d+2}^t) \\ &= (f(s_{t-d}, x_{t-d+1}, y_{t-d+1}), x_{t-d+2}^t) \\ &\triangleq \tilde{f}(\tilde{s}_{t-1}, \tilde{x}_t, \tilde{y}_t), \end{aligned}$$

where, clearly,  $\tilde{f} : \tilde{\mathcal{X}} \times \tilde{\mathcal{Y}} \times \tilde{\mathcal{S}} \rightarrow \tilde{\mathcal{S}}$  is a time-invariant function of  $(\tilde{s}_{t-1}, \tilde{x}_t, \tilde{y}_t)$ . Thus, the unifilar property holds in this case.

- Conditioned on the previous channel state  $\tilde{S}_{t-1}$  and the channel input  $\tilde{X}_t$ , the channel output  $\tilde{Y}_t$  is independent of any other previous states, inputs, and outputs. Specifically, note that  $\tilde{s}_{t-1}$  includes the pair  $(s_{t-d}, x_{t-d+1})$ , and therefore it implies that

$$P(\tilde{y}_t | \tilde{x}^t, \tilde{y}^{t-1}, \tilde{s}^{t-1}) = P(\tilde{y}_t | \tilde{x}_t, \tilde{s}_{t-1}),$$

due to the fact that the redefined channel output  $\tilde{y}_t$  is the original channel output at time  $(t-d+1)$ .

- The initial state  $\tilde{S}_0$  is known both to the encoder and to the decoder, as required. As shown above, the redefined channel is a FSC. Additionally, at each time-step  $t$ , the encoder knows all previous channel outputs  $\tilde{y}^{t-1}$ , as required in the case of instantaneous feedback.

We note that following our proposed transformation, the decoder does not have access to the last  $d$  channel outputs. Thus, the resulting capacity of the transformed channel is a lower bound on the delayed feedback capacity of the original channel. However, this reduction in the block length has a vanishing effect on the limiting capacity as  $d$  is assumed to be finite while  $n$  grows large. Now, given an input sequence, the corresponding outputs of the redefined FSC are drawn according to the statistics of the original channel model. Furthermore, maximizing over  $P(\tilde{x}^n | \tilde{y}^{n-1})$  is equivalent to maximizing over  $P(x^n | y^{n-d})$ . Therefore, we can deduce that the capacity of the original channel with delayed feedback can be computed as

$$C_d^{\text{fb}} = \lim_{n \rightarrow \infty} \max_{P(\tilde{x}^n | \tilde{y}^{n-1})} \frac{1}{n} I(\tilde{X}^n \rightarrow \tilde{Y}^n), \quad (12)$$

while reformulating the channel model as described above.

A similar formulation appeared in [41], [42], but only for the case where the channel state  $s_t$  is a deterministic function of  $s_{t-1}$  and  $x_t$ . Here, we presented a general formulation that holds for any FSC. The trapdoor channel, for instance, does not fall into the framework of [41] and [42] since the channel state depends on the channel outputs as well.

**Remark 5.** Following our formulation, it is interesting to observe that the channel output  $\tilde{Y}_t$  is independent of  $\tilde{X}_t$  conditioned on  $\tilde{S}_{t-1}$ . In other words, the channel output solely depends on the channel state and not on the channel input. However, the choice of the channel input  $\tilde{x}_t$  is still of significant importance since it directly affects the evolution of the next channel state.

□

### B. $Q$ -graph Bounds on Delayed Feedback Capacity

In Section III we introduced two powerful methodologies to compute upper and lower bounds on the capacity of unifilar FSCs with instantaneous feedback. Based on these approaches, we establish computable upper and lower bounds on the capacity of the unifilar FSC with delayed feedback. Specifically, following Theorem 7, since the delayed feedback capacity of a unifilar FSC can be computed as the capacity of a new unifilar FSC with instantaneous feedback, the computable bounds from Section III can be directly adapted for the case of delayed feedback, just by redefining the channel and then applying the bounds on the new unifilar FSC. We emphasize that a delay of at least two time instances is assumed here. Otherwise, we have the standard instantaneous feedback scenario. In the following theorem, we present the  $Q$ -graph lower bound for the case of delayed feedback.

**Theorem 8.** *If the initial state  $\tilde{s}_0$  is available to both the encoder and the decoder, then the  $d$  time instances delayed feedback capacity of a strongly connected unifilar FSC is bounded by*

$$C_d^{\text{fb}} \geq I(\tilde{S}; \tilde{Y}|Q), \quad (13)$$

where  $\tilde{X}$ ,  $\tilde{Y}$ ,  $\tilde{S}$  are the new channel input, output, and state, respectively (as defined in Section IV-A). The bound holds only for aperiodic inputs  $P_{\tilde{X}|\tilde{S},Q} \in \mathcal{P}_\pi$  that are BCJR-invariant, and for all irreducible  $Q$ -graphs with  $q_0$  such that  $(\tilde{s}_0, q_0)$  lies in an aperiodic closed communicating class.

Following Remark 2, it is evident that any graph-based encoder (comprising of a  $Q$ -graph and a BCJR input distribution) for the delayed feedback capacity problem provides a lower bound (Theorem 8) and a coding scheme that achieve this lower bound. The construction details of the coding scheme are precisely given in [19], [22], where the new transformed channel is considered for the construction. Further, the  $Q$ -graph upper bound for the case of delayed feedback is given in the theorem below.

**Theorem 9.** *The  $d$  time instances delayed feedback capacity of a strongly connected unifilar FSC, where the initial state is available to both the encoder and the decoder, is bounded by*

$$C_d^{\text{fb}} \leq \sup_{P_{\tilde{X}|\tilde{S},Q} \in \mathcal{P}_\pi} I(\tilde{S}; \tilde{Y}|Q), \quad (14)$$

where  $\tilde{X}$ ,  $\tilde{Y}$ ,  $\tilde{S}$  are the new channel input, output, and state, respectively (as defined in Section IV-A). The bound holds for all  $Q$ -graphs for which the  $(\tilde{S}, Q)$ -graph has a single and aperiodic closed communicating class. The joint distribution is  $P_{\tilde{Y},\tilde{X},\tilde{S},Q} = P_{\tilde{Y}|\tilde{X},\tilde{S}} P_{\tilde{X}|\tilde{S},Q} \pi_{\tilde{S},Q}$ , where  $\pi_{\tilde{S},Q}$  is the stationary distribution of the  $(\tilde{S}, Q)$ -graph.

*Proof of Theorems 9 and 8.* First, as shown in Section IV-A, after reformulating the FSC, we obtain an equivalent instantaneous feedback capacity problem. Since the new induced channel is a unifilar FSC, Theorems 3 and 4 can be directly applied on the new unifilar channel. Accordingly, it is only left to show

that it is sufficient to optimize  $I(\tilde{S}; \tilde{Y}|Q)$  instead of  $I(\tilde{X}, \tilde{S}; \tilde{Y}|Q)$ . The latter holds by the trivial Markov chain  $\tilde{Y} - \tilde{S} - \tilde{X}$ . In particular, according to the new formulation, the new channel state already include the new channel input.  $\square$

## V. TRAPDOOR CHANNEL WITH DELAYED FEEDBACK

The trapdoor channel (Fig. 2) has had a long history in information theory since its introduction by David Blackwell in 1961 [29]. The channel has attracted much interest since its representation is very simple, yet its capacity computation is highly non-trivial. The channel can be viewed as a (causal) permutation channel since the weight of the input sequence is equal to the weight of the output sequence. This channel is also termed the *chemical channel*, which alludes to a physical system in which chemical concentrations are used to communicate [43]. A detailed discussion on the trapdoor channel can be found in Robert Ash's book [44] (which even uses the channel for his book cover).

The trapdoor channel is a unifilar FSC whose operation can be described as follows. At time  $t$ , let  $x_t \in \{0, 1\}$  be the channel input and  $s_{t-1} \in \{0, 1\}$  be the previous channel state. The channel input,  $x_t$ , is transmitted through the channel. The channel output,  $y_t$ , is equal to the previous state  $s_{t-1}$  or to the input  $x_t$ , with the same probability. The new channel state is evaluated according to  $s_t = x_t \oplus y_t \oplus s_{t-1}$ , where  $\oplus$  denotes the XOR operation.

Although the capacity of the trapdoor channel without feedback is unknown, it is known in two important variations of the original capacity problem. In [24], [25], it was shown that the zero-error capacity of the trapdoor channel is  $C_0 = 0.5$  bits per channel use. This provides a lower bound on the feedforward capacity which is known to be non-tight (e.g. [26]). The other variation is the feedback capacity, which is equal to  $C_1^{\text{fb}} = \log_2 \left( \frac{1+\sqrt{5}}{2} \right) \approx 0.6942$ , as shown in [12]. It is also known that feedback *does increase* the capacity for the trapdoor channel (e.g. [27], [28]).

The following theorem states our main result concerning the delayed feedback capacity of the trapdoor channel.

**Theorem 10.** *The capacity of the trapdoor channel with delayed feedback of two time instances is*

$$C_2^{\text{fb}} = \log_2 \left( \frac{3}{2} \right).$$

The proof of Theorem 10 is given in Appendix A. This result concludes the delayed feedback capacity, and we will now discuss several implications of our capacity result. The above capacity is approximately  $C_2^{\text{fb}} \approx 0.5849$ , while the instantaneous feedback capacity is approximately  $C_1^{\text{fb}} \approx 0.6942$ . The best lower bound to date on the feedforward capacity is  $C \geq 0.572$  [26]. It is interesting to note that even a single time-instance delay leads to a sharp decrease in the capacity towards the feedforward capacity.

The delayed feedback capacity in Theorem 10 also serves as an upper bound on the feedforward capacity. Overall, the best bounds on the feedforward capacity are given by

$$0.572 \leq C \leq 0.5849.$$

While the delayed feedback capacity is equal to the best upper bound on the feedforward capacity, it does not establish a new upper bound. In particular, a recent paper proposed using duality-based upper bounds on the feedforward capacity and established the same bound [28]. However, their bound is for the feedforward capacity only, and therefore we still need to show a converse proof for Theorem 10.

An interesting question is whether the delayed feedback capacity is, indeed, the feedforward capacity. Simulations of the delayed feedback capacity with a delay greater than two time instances suggest that this is not the case. In particular, by operational considerations, we have the following chain of inequalities:

$$C \leq \dots \leq C_3^{\text{fb}} \leq C_2^{\text{fb}} \leq C_1^{\text{fb}}. \quad (15)$$

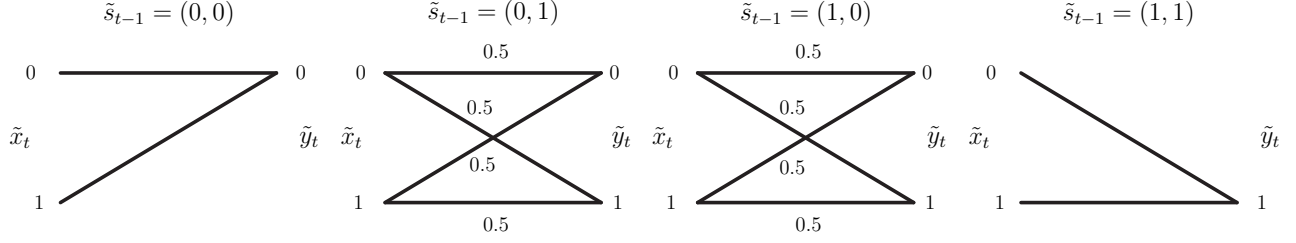


Fig. 5. The trapdoor channel with delayed feedback of two time instances as a new unifilar FSC with instantaneous feedback.

As clarified, the upper bound in Theorem 9 can be formulated as a convex optimization problem, and its evaluation for a greater delay of the feedback gives

$$C_3^{\text{fb}} \leq 0.5782, \quad C_4^{\text{fb}} \leq 0.5765. \quad (16)$$

Accordingly, these simulations suggest that the feedforward capacity satisfies  $C \leq 0.5765$ . In other words, the delayed feedback capacity in Theorem 10 does not seem to be the feedforward capacity, which remains an open problem.

**Remark 6.** The achievability proof of Theorem 10 is based on the  $Q$ -graph lower bound, which was presented in Section IV-B. That is, the lower bound was established by showing that a particular graph-based encoder, given by the  $Q$ -graph in (25) and the input distribution in (26), provides an achievable rate of  $\log_2(3/2)$ . This graph-based encoder implies a simple coding scheme that, in our case, achieves the capacity. As explained in Remark 2, the scheme is based on the posterior matching principle, and the exact details regarding the construction of the coding scheme are given in [22].

**Remark 7.** Following the formulation in Section IV-A, we present in Fig. 5 the trapdoor channel with delayed feedback of two time instances as a new unifilar FSC with instantaneous feedback. For the new FSC, it is interesting to note that the capacity of each individual channel (per state) is zero. Nevertheless, as we already demonstrated, the capacity of the overall FSC is not zero. This follows due to the fact that, at each time  $t$ , the output depends only on the previous channel state, and the choice of the current input will only participate in the evolution of the next channel state.

## VI. UPPER BOUNDS ON FEEDFORWARD CAPACITY

In this section, we demonstrate that the investigation of the delayed feedback capacity plays an important role in deriving upper bounds on the feedforward capacity. Specifically, besides the trapdoor channel, we present here two additional FSCs for which we derive novel results concerning their feedforward capacity by investigating their delayed feedback capacity. It is important to note that as the delay  $d$  grows, the upper bounds on the feedforward capacity may improve. In practice, we show that even small values of  $d \geq 2$  lead to very good upper bounds when compared to corresponding lower bounds on the feedforward capacity. Thus, an instantaneous feedback is significant in terms of capacity.

### A. Input-Constrained BSC

Regardless of whether feedback is allowed or not, memoryless channels have the same simple single-letter capacity expression [45]. When the inputs are constrained, however, the capacity problem is very challenging. The feedforward capacity in the presence of constrained inputs has been extensively investigated, e.g. [30], [32], [33], [46], [47], but is still given by a multi-letter expression.

Here, we consider the BSC with crossover probability  $p$ , denoted by  $\text{BSC}(p)$ , where the inputs are constrained to satisfy the  $(1, \infty)$ -RLL constraint. Namely, the input sequence does not contain two consecutive ones. Even though this setting does not fall under the classical definition of a unifilar FSC,

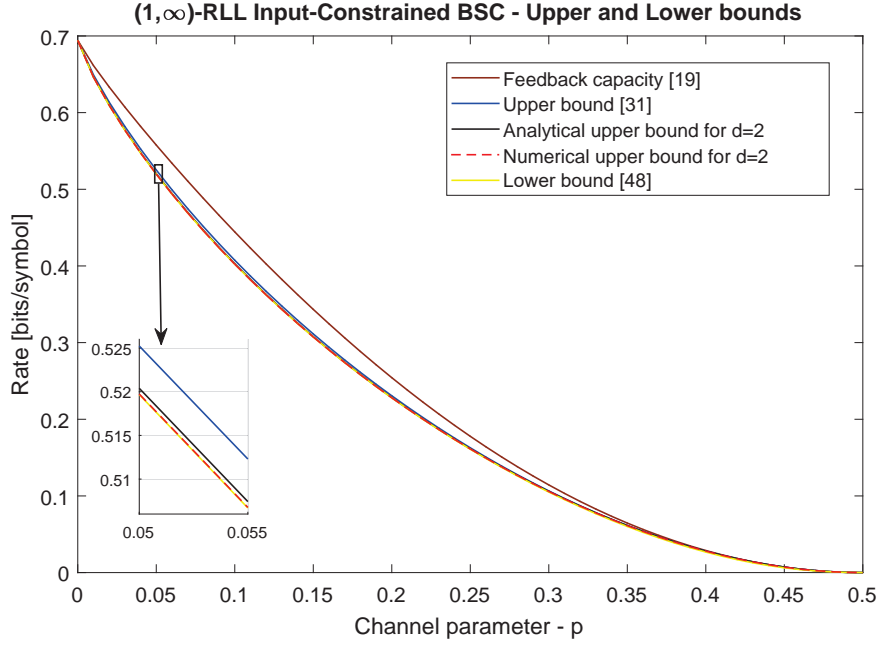


Fig. 6. Upper and lower bounds on the feedforward capacity of the input-constrained BSC( $p$ ). The top brown line is the feedback capacity from [19]. The blue line is the best known upper bound on the feedforward capacity from [31]. The black line represents our analytical upper bound on the delayed feedback capacity from Theorem 11. The red line represents a numerical upper bound on the delayed feedback capacity, which was evaluated using a 3-order Markov  $Q$ -graph. Finally, the bounds are compared to a lower bound on the feedforward capacity (yellow line).

it is straightforward to convert input constraints by defining a dummy sink state whose capacity is zero in the case that the constraint is violated. For this setting, while the feedforward capacity is still open, the feedback capacity was established in [19], and it is known that feedback does increase the capacity [19], [31].

In the theorem below we present a novel result concerning the capacity of the BSC with a no consecutive ones input constraint.

**Theorem 11.** *The capacity of the input-constrained BSC( $p$ ) with a  $(1, \infty)$ -RLL constraint and delayed feedback of two time instances satisfies*

$$C_2^{\text{fb}}(p) \leq \min \log_2 \left( \frac{p^p \bar{p}^{\bar{p}} a^{(p^3-3p^2+3p-1)} (\bar{b}\bar{c}\bar{d})^{(p^3-p^2)}}{(\bar{a}bc)^{(p^3-2p^2+p)} \bar{d}p^3} \right),$$

where the minimum is over all  $(a, b, c, d) \in [0, 1]^4$  that satisfy:

$$\begin{aligned} 1 &\leq \frac{a^{(4p^3-12p^2+11p-3)} (\bar{b}\bar{d})^{(4p^3-6p^2+2p)} \bar{c}^{(4p^3-4p^2+p)}}{(\bar{a}\bar{c})^{(4p^3-8p^2+5p-1)} b^{(4p^3-10p^2+6p-1)} \bar{d}^{(4p^3-2p^2)}}, \\ 1 &\leq \frac{a^{(4p^3-10p^2+8p-2)} (\bar{b}\bar{d})^{(4p^3-4p^2+p)} \bar{c}^{(4p^3-2p^2-2p+1)}}{(\bar{a}\bar{c})^{(4p^3-6p^2+2p)} b^{(4p^3-8p^2+5p-1)} \bar{d}^{(4p^3-p)}}. \end{aligned} \quad (17)$$

The proof of Theorem 11 is given in Appendix B.

In Fig. 6, the delayed feedback capacity upper bound in Theorem 11 is plotted along with the feedback capacity from [19], the best upper bound on the feedforward capacity from [31], a numerical upper bound on the delayed feedback capacity of two time instances, and a lower bound on the feedforward capacity obtained using the simulation method in [48]. Here as well, it is surprising to note from the plot

that the difference between the capacity with instantaneous feedback and the capacity with an additional time-instance delay is quite significant. Further, although our analytical upper bound in Theorem 11 was introduced for the case of delayed feedback, it also serves as a novel upper bound on the feedforward capacity, and outperforms all previously known bounds. Nonetheless, our upper bound almost coincides with the lower bound on the feedforward capacity.

We would like to emphasize that our upper bound in Theorem 11 can be further improved. Specifically, the dashed red line in Fig. 6 was obtained by evaluating the upper bound in Theorem 9 with a 3-order Markov  $Q$ -graph, which consist of eight nodes, and its evolution function is given by the vector representation

$$\begin{aligned}\underline{\phi}(\underline{q}, \tilde{y} = 0) &= [1, 3, 5, 7, 1, 3, 5, 7] \\ \underline{\phi}(\underline{q}, \tilde{y} = 1) &= [2, 4, 6, 8, 2, 4, 6, 8].\end{aligned}\tag{18}$$

This vector representation implies, for instance,  $\phi(q = 1, \tilde{y} = 0) = 1$  and  $\phi(q = 1, \tilde{y} = 1) = 2$ . It can be noted from the figure that the induced upper bound provides an even tighter bound on the delayed feedback capacity of two time instances. However, the upper bound in Theorem 11 already achieves remarkable performance, and therefore we do not provide here an analytical expression for the additional bound.

### B. The Dicode Erasure Channel

The DEC was studied in [21], [28], [34], [35] and is a simplified version of the well-known dicode channel with additive white Gaussian noise. The operation of the DEC is illustrated in Fig. 3. The feedback capacity of the DEC was established in [21], and is given in the theorem below. However, in the absence of feedback the capacity is still unknown.

**Theorem 12** ([21], Th. 5). *The feedback capacity of the DEC is*

$$C_1^{\text{fb}}(p) = \max_{\epsilon \in [0,1]} (1-p) \frac{\epsilon + p H_2(\epsilon)}{p + (1-p)\epsilon} \tag{19}$$

for any channel parameter  $p \in [0, 1]$ .

In the following theorem, we derive an upper bound on the delayed feedback capacity of the DEC for  $p = 0.5$ . This bound serves as a novel upper bound on the feedforward capacity, and it also demonstrates that feedback does increase the capacity of the DEC for  $p = 0.5$ .

**Theorem 13.** *The capacity of the DEC with delayed feedback of two time instances is upper bounded by*

$$C_2^{\text{fb}}(0.5) \leq \max_{a \in (0,0.5)} \frac{1}{4} \cdot \log_2 \left( \frac{2 - 3a}{(1 - 2a) \cdot (1 + 8a^2\bar{a} - 3a - (1 - 4a\bar{a})\sqrt{1 + 4a^3})} \right).$$

The proof of Theorem 13 is given in Appendix C. The upper bound is derived by using a particular  $Q$ -graph with eight nodes, which is given within the proof of the theorem.

In Fig. 7, we present bounds on the feedforward capacity of the DEC. In particular, the red line is the feedback capacity from Theorem 12, which serves as a non-trivial upper bound. The black line is an achievable rate from [49], obtained by considering a first-order Markov input process. Finally, the blue line shows our upper bound on the two time instances delayed feedback capacity. This bound is a numerical evaluation of Theorem 9 with the same  $Q$ -graph that is used for the proof of Theorem 13. Accordingly, for  $p = 0.5$ , the plot provides a numerical evaluation of the analytical upper bound in Theorem 13. In [28], the authors derived an upper bound on the feedforward capacity, which turned out to be exactly equal to the feedback capacity. This fact led to the question of whether the feedback capacity is equal to the feedforward capacity, which, indeed, is negligibly different from the first-order Markov achievable

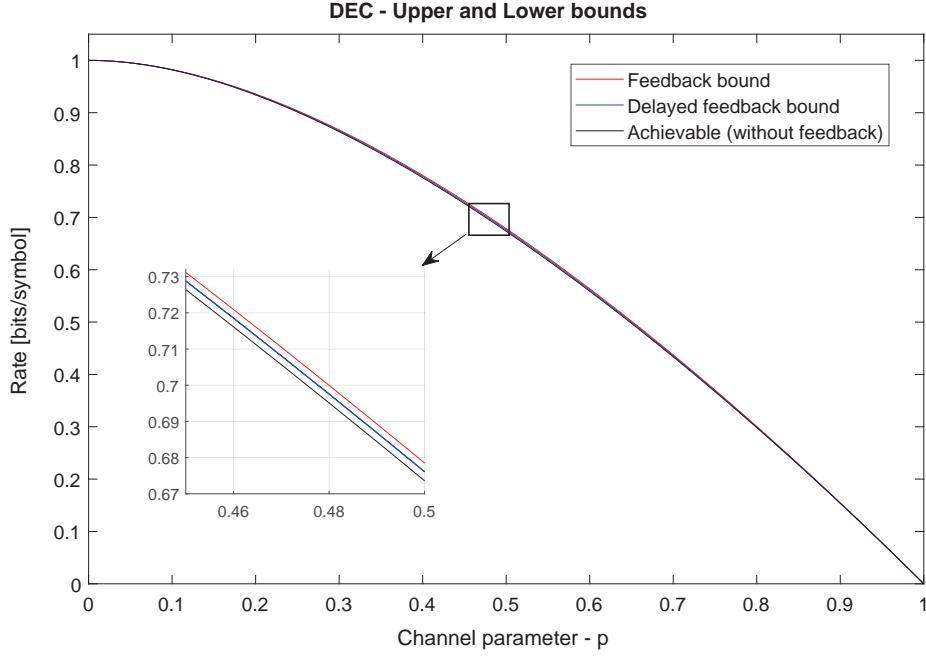


Fig. 7. Upper and lower bound on the capacity of the DEC. The feedback bound is the feedback capacity from [21]. The delayed feedback bound (blue line) is our upper bound. The black line is an achievable rate on the feedforward capacity.

rate. Following our numerical upper bound, we could see that this bound improves the feedback capacity for any  $p \in (0, 1)$ , which indicates that feedback increases the capacity of the DEC over the entire region of the erasure parameter.

## VII. CONCLUSIONS

In this paper, we investigated the delayed feedback capacity of FSCs. It was shown that the capacity of a FSC with delayed feedback can be computed as that of a new FSC with instantaneous feedback. Accordingly, several graph-based methods to obtain computable bounds on the capacity of unifilar FSCs, which were introduced for the case of instantaneous feedback, could be adapted to the case of delayed feedback as well. Using these bounds, we could establish that the capacity of the trapdoor channel with delayed feedback of two time instances is equal to  $\log_2(\frac{3}{2})$ . In addition, we derived an upper bound on the delayed feedback capacity of the input-constrained BSC, which also serves as a novel upper bound on its feedforward capacity. Finally, we demonstrate that feedback increases capacity for the DEC.

## APPENDIX A

### TRAPDOOR CHANNEL — PROOF OF CAPACITY (THEOREM 10)

*Proof.* The proof of the capacity result in Theorem 10 consists of two parts. In Section A-A, we prove the converse, that is,  $C_2^{\text{fb}} \leq \log_2(\frac{3}{2})$ , and in Section A-B, we show a corresponding lower bound. The proof is based on the methodology in Section III. As clarified, the upper and lower bounds hold for instantaneous feedback, but using the formulation in Section IV-A, we are able to transform the delayed feedback capacity into a capacity problem with instantaneous feedback.

We begin with presenting the formulation of the trapdoor channel with delayed feedback as a new unifilar FSC with instantaneous feedback. The new FSC (see Fig. 5) is defined as follows: the channel state consists of the pair of the previous channel state and channel input, that is,  $\tilde{s}_{t-1} \triangleq (s_{t-2}, x_{t-1})$ . The channel input is  $\tilde{x}_t = x_t$  and the channel output is  $\tilde{y}_t = y_{t-1}$ . If  $\tilde{s}_{t-1} = (0, 1)$  or  $\tilde{s}_{t-1} = (1, 0)$ , then we have a BSC(0.5). Otherwise, for any  $\tilde{x}_t$ , if  $\tilde{s}_{t-1} = (0, 0)$  then  $\tilde{y}_t = 0$ , and if  $\tilde{s}_{t-1} = (1, 1)$  then  $\tilde{y}_t = 1$ .

### A. Upper Bound

Here, we will show that  $C_2^{\text{fb}} \leq \log_2\left(\frac{3}{2}\right)$ . The proof is based on fixing a particular graph-based test distribution, and then solving the MDP problem of the dual capacity upper bound (for additional details, see Section III-B). The MDP formulation is presented in Table I.

Consider the  $Q$ -graph in Fig. 4, which consists of two nodes, and the following graph-based test distribution:

$$T(\tilde{y} = 0|\underline{q}) = \left[\frac{2}{3}, \frac{1}{3}\right]. \quad (20)$$

To present the solution for the Bellman equation, define the constant

$$\rho^* = \log_2\left(\frac{3}{2}\right), \quad (21)$$

and the value function

$$h(\tilde{s}, q) = \begin{cases} 1, & (\tilde{s} = (0, 0), q = 2) \text{ or } (\tilde{s} = (1, 1), q = 1), \\ 0, & \text{else.} \end{cases} \quad (22)$$

**Remark 8.** The conjectured solution  $(\rho^*, h(\cdot))$  has been obtained by using the value iteration algorithm with the MDP defined in Table I. Specifically, applying the value iteration algorithm provides the optimal policy for any possible MDP state. Then, it is only left to solve a finite set of linear equations in order to derive closed-form expressions for  $\rho^*$  and  $h(\cdot)$ .

We proceed to show that  $\rho^*$  in (21) and the value function in (22) solve the Bellman equation. This directly implies, by Theorem 5, that  $C_2^{\text{fb}} \leq \rho^* = \log_2(3/2)$ . For the MDP state  $(\tilde{s} = (0, 0), q = 1)$ , the right-hand side of the Bellman equation is a maximum over  $\tilde{x}$  of

$$\begin{aligned} & D\left(P_{\tilde{Y}|\tilde{X}, \tilde{S}}(\cdot|\tilde{x}, \tilde{s}) \parallel T_{\tilde{Y}|Q}(\cdot|q)\right) + \sum_{\tilde{y} \in \mathcal{Y}} P(\tilde{y}|\tilde{x}, \tilde{s}) h\left(\tilde{f}(\tilde{s}, \tilde{x}, \tilde{y}), \phi(q, \tilde{y})\right) \\ & \stackrel{(a)}{=} \begin{cases} D\left([1, 0] \parallel \left[\frac{2}{3}, \frac{1}{3}\right]\right) + h((0, 0), 1), & \text{if } \tilde{x} = 0, \\ D\left([1, 0] \parallel \left[\frac{2}{3}, \frac{1}{3}\right]\right) + h((0, 1), 1), & \text{if } \tilde{x} = 1. \end{cases} \\ & \stackrel{(b)}{=} \log_2\left(\frac{3}{2}\right), \quad \text{for all } \tilde{x} \end{aligned} \quad (23)$$

where (a) follows by the channel definition and our choice of the test distribution, and (b) follows since according to (22) we have  $h((0, 0), 1) = h((0, 1), 1) = 0$ , and also  $D\left([1, 0] \parallel \left[\frac{2}{3}, \frac{1}{3}\right]\right) = \log_2(3/2)$ . Further, the left-hand side of the Bellman equation is  $\rho^* + h((0, 0), 1)$ , which is equal to  $\log_2\left(\frac{3}{2}\right)$  as well. Therefore, we can conclude that the Bellman equation holds for  $(\tilde{s} = (0, 0), q = 1)$ .

For the MDP state  $(\tilde{s} = (0, 0), q = 2)$ , the right-hand side of the Bellman equation is a maximum over  $\tilde{x}$  of

$$\begin{aligned} & D\left(P_{\tilde{Y}|\tilde{X}, \tilde{S}}(\cdot|\tilde{x}, \tilde{s}) \parallel T_{\tilde{Y}|Q}(\cdot|q)\right) + \sum_{\tilde{y} \in \mathcal{Y}} P(\tilde{y}|\tilde{x}, \tilde{s}) h\left(\tilde{f}(\tilde{s}, \tilde{x}, \tilde{y}), \phi(q, \tilde{y})\right) \\ & = \begin{cases} D\left([1, 0] \parallel \left[\frac{1}{3}, \frac{2}{3}\right]\right) + h((0, 0), 2), & \text{if } \tilde{x} = 0, \\ D\left([1, 0] \parallel \left[\frac{1}{3}, \frac{2}{3}\right]\right) + h((0, 1), 2), & \text{if } \tilde{x} = 1. \end{cases} \end{aligned} \quad (24)$$

Also here, in both cases of  $\tilde{x}$ , the equation is equal to  $\log_2(3)$ , while the left-hand side of the Bellman equation is  $\rho^* + h((0, 0), 2) = \log_2(3)$ . Thus, the Bellman equation holds for this case too. The verification for the remaining MDP states can be done similarly.



### B. Lower Bound

The lower bound is derived using Theorem 8 with a particular graph-based encoder that induces the BCJR-invariant property. We show that the achievable rate induced by the graph-based encoder is  $R = \log_2 \left( \frac{3}{2} \right)$ , and therefore  $C \geq \log_2 \left( \frac{3}{2} \right)$ .

A graph-based encoder consists of a  $Q$ -graph and an input distribution  $P_{X|S,Q}$  that is BCJR-invariant. We choose a  $Q$ -graph consisting of four nodes, and its evolution function is given by the vector representation

$$\begin{aligned}\underline{\phi}(\underline{q}, \tilde{y} = 0) &= [1, 3, 1, 3] \\ \underline{\phi}(\underline{q}, \tilde{y} = 1) &= [2, 4, 2, 4].\end{aligned}\tag{25}$$

For the  $Q$ -graph in (25), we define the following input distribution:

$$P_{\tilde{X}|\tilde{S},Q}(0|\tilde{s}, q) = \begin{array}{c|cccc} & \tilde{s} = (0, 0) & \tilde{s} = (0, 1) & \tilde{s} = (1, 0) & \tilde{s} = (1, 1) \\ \hline q = 1 & 2/3 & 1/3 & 1/3 & 0 \\ q = 2 & 1 & 2/3 & 0 & 1/3 \\ q = 3 & 2/3 & 1 & 1/3 & 0 \\ q = 4 & 1 & 2/3 & 2/3 & 1/3 \end{array}.\tag{26}$$

According to (3), the Markov transition probability can now be computed as

$$P(\tilde{s}^+, q^+|\tilde{s}, q) = \sum_{\tilde{x}, \tilde{y}} P(\tilde{x}|\tilde{s}, q) P(\tilde{y}|\tilde{x}, \tilde{s}) \mathbb{1}_{\{q^+ = \phi(q, \tilde{y})\}} \mathbb{1}_{\{\tilde{s}^+ = \tilde{f}(\tilde{s}, \tilde{x}, \tilde{y})\}}.$$

Consequently, standard computation of the stationary distribution  $\pi(\tilde{s}, q)$  provides that

$$\pi_{\tilde{S},Q}(\tilde{s}, q) = \begin{array}{c|cccc} & \tilde{s} = (0, 0) & \tilde{s} = (0, 1) & \tilde{s} = (1, 0) & \tilde{s} = (1, 1) \\ \hline q = 1 & 1/6 & 1/12 & 1/36 & 1/18 \\ q = 2 & 1/36 & 1/18 & 0 & 1/12 \\ q = 3 & 1/12 & 0 & 1/18 & 1/36 \\ q = 4 & 1/18 & 1/36 & 1/12 & 1/6 \end{array}.$$

We now verify that the proposed graph-based encoder satisfies the BCJR-invariant property in (5). Let us show this explicitly for the case where  $(q, \tilde{y}) = (1, 1)$  and  $\tilde{s}^+ = (0, 0)$ . Since  $\phi(1, 1) = 2$ , the left-hand side of Eq. (5) is equal to  $\pi_{\tilde{S}|Q}((0, 0)|2)$ , while the right-hand side is equal to

$$\begin{aligned}& \frac{\sum_{x,s} \pi_{\tilde{S}|Q}(s|1) P_{\tilde{X}|\tilde{S},Q}(x|s, 1) P_{\tilde{Y}|\tilde{X},\tilde{S}}(1|x, s) \mathbb{1}_{\{(0,0)=\tilde{f}(x,1,s)\}}}{\sum_{x',s'} \pi_{\tilde{S}|Q}(s'|1) P_{\tilde{X}|\tilde{S},Q}(x'|s', 1) P_{\tilde{Y}|\tilde{X},\tilde{S}}(1|x', s')} \\ &= \frac{1}{6},\end{aligned}$$

which, indeed, is equal to  $\pi_{\tilde{S}|Q}((0, 0)|2)$ , as required. The verification of the other cases can be done similarly.

Finally, the achievable rate of the graph-based encoder is

$$\begin{aligned}R &= I(\tilde{S}; \tilde{Y}|Q) \\ &= \sum_{q \in \mathcal{Q}} \pi_Q(q) \cdot I(\tilde{S}; \tilde{Y}|Q = q) \\ &= \sum_{q \in \mathcal{Q}} \pi_Q(q) \cdot \left[ H_2(\tilde{Y}|Q = q) - H_2(\tilde{Y}|\tilde{S}, Q = q) \right] \\ &\stackrel{(a)}{=} \sum_{q \in \mathcal{Q}} \pi_Q(q) \cdot \left[ H_2\left(\frac{2}{3}\right) - H_2(\tilde{Y}|\tilde{S}, Q = q) \right]\end{aligned}$$

$$\begin{aligned}
&= H_2\left(\frac{2}{3}\right) - \sum_{q \in \mathcal{Q}} \pi_Q(q) \cdot H_2(\tilde{Y}|\tilde{S}, Q=q) \\
&= H_2\left(\frac{2}{3}\right) - \frac{1}{3} \\
&= \log_2\left(\frac{3}{2}\right),
\end{aligned}$$

where (a) follows due to the fact that

$$\begin{aligned}
P_{\tilde{Y}|Q}(0|q) &= \sum_{\tilde{x}, \tilde{s}} \pi(\tilde{s}|q) P(\tilde{x}|\tilde{s}, q) P_{\tilde{Y}|\tilde{X}\tilde{S}}(0|\tilde{x}, \tilde{s}) \\
&= \begin{cases} 2/3, & q = 1 \text{ or } q = 3, \\ 1/3, & q = 2 \text{ or } q = 4. \end{cases}
\end{aligned}$$

□

## APPENDIX B

### INPUT-CONSTRAINED BSC — PROOF OF THEOREM 11

*Proof.* Here we provide the proof of Theorem 11 regarding the upper bound on the capacity of the  $(1, \infty)$ -input constrained BSC( $p$ ). We begin with the formulation of the channel with delayed feedback of two time instances as a new unifilar FSC with instantaneous feedback. The channel state is defined as  $\tilde{s}_{t-1} \triangleq (x_{t-2}, x_{t-1})$ , the channel input is  $\tilde{x}_t = x_t$ , and the channel output is  $\tilde{y}_t = y_{t-1}$ . If  $\tilde{s}_{t-1} = (0, 0)$  or  $\tilde{s}_{t-1} = (1, 0)$ , then  $\tilde{y}_t = 0$  with probability  $1 - p$  or  $\tilde{y}_t = 1$  with probability  $p$ . Otherwise, if  $\tilde{s}_{t-1} = (0, 1)$ , then  $\tilde{y}_t = 0$  with probability  $p$  or  $\tilde{y}_t = 1$  with probability  $1 - p$ . Due to the input constraint, if  $\tilde{s}_{t-1} = (0, 1)$ , then the transmitted input  $\tilde{x}_t$  must be zero.

For a particular graph-based test distribution, we solve the MDP problem of the dual capacity upper bound. Here too, consider the  $Q$ -graph in Eq. (25), and the following parameterized graph-based test distribution:

$$T(\tilde{y} = 0|\underline{q}) = [a, b, c, d], \quad (27)$$

where  $(a, b, c, d) \in (0, 1)^4$ . Define the constant

$$\rho^* = \log_2 \left( \frac{p^p \bar{p}^{\bar{p}} a^{(p^3 - 3p^2 + 3p - 1)} (\bar{b} \bar{c} \bar{d})^{(p^3 - p^2)}}{(\bar{a} \bar{b} \bar{c})^{(p^3 - 2p^2 + p)} \bar{d}^{p^3}} \right). \quad (28)$$

Further, define the value function  $h(\tilde{s}, q)$  as follows:

$$\begin{aligned}
h((0, 0), 1) &= h((1, 0), 1) = \log_2 \left( \frac{\bar{c}^p d \bar{d}^p c^{1-2p}}{\bar{a}^{2p} b^p a^{2-3p}} \cdot \left( \frac{\bar{a} b c \bar{d}}{\bar{a} \bar{b} \bar{c} \bar{d}} \right)^{p^2} \right) \\
h((0, 0), 2) &= h((1, 0), 2) = \log_2 \left( \frac{d}{b} \cdot \left( \frac{b \bar{d}}{\bar{b} d} \right)^p \right) \\
h((0, 0), 3) &= h((1, 0), 3) = \log_2 \left( \frac{a^{2p-1} d \bar{d}^p}{(\bar{a} \bar{b} \bar{c})^p} \cdot \left( \frac{\bar{a} b c \bar{d}}{\bar{a} \bar{b} \bar{c} \bar{d}} \right)^{p^2} \right) \\
h((0, 0), 4) &= h((1, 0), 4) = 0 \\
h((0, 1), 1) &= \log_2 \left( \frac{a^{6p^2-6p+1} \bar{b}^{2p^2-p} \bar{c}^{2p^2} d^{2p^2-p+1} \bar{d}^p}{\bar{a}^{4p^2-2p+1} b^{4p^2-3p+1} c^{4p^2-2p}} \cdot \left( \frac{\bar{a} b c \bar{d}}{\bar{a} \bar{b} \bar{c} \bar{d}} \right)^{2p^3} \right)
\end{aligned}$$

$$\begin{aligned}
h((0, 1), 2) &= \log_2 \left( \frac{a^{5p^2-4p+1}(\bar{a}cd)^p(\bar{b}\bar{c}d\bar{d})^{p^2}}{\bar{b}^{1-p}(\bar{a}bc)^{3p^2}} \cdot \left( \frac{\bar{a}bcd}{\bar{a}\bar{b}\bar{c}\bar{d}} \right)^{2p^3} \right) \\
h((0, 1), 3) &= \log_2 \left( \frac{a^{6p^2-5p+1}\bar{b}^{2p^2-p}\bar{c}^{2p^2+p-1}d^{2p^2-p+1}\bar{d}^p}{\bar{a}^{4p^2-p}\bar{b}^{4p^2-3p+1}c^{4p^2-p}} \cdot \left( \frac{\bar{a}bcd}{\bar{a}\bar{b}\bar{c}\bar{d}} \right)^{2p^3} \right) \\
h((0, 1), 4) &= \log_2 \left( \frac{a^{5p^2-4p+1}(\bar{b}\bar{c}d\bar{d})^{p^2}}{(\bar{a}bc)^{3p^2-p}\bar{d}^{1-p}} \cdot \left( \frac{\bar{a}bcd}{\bar{a}\bar{b}\bar{c}\bar{d}} \right)^{2p^3} \right).
\end{aligned} \tag{29}$$

To complete the proof it is left to show that, under the constraints given in (17), the scalar  $\rho^*$  in (28) and the value function in (29) solve the Bellman equation. For the MDP state  $(\tilde{s} = (0, 0), q = 1)$ , the right-hand side of the Bellman equation is a maximum over  $\tilde{x}$  of

$$\begin{aligned}
& D\left(P_{\tilde{Y}|\tilde{X},\tilde{S}}(\cdot|\tilde{x},\tilde{s})\left\|T_{\tilde{Y}|Q}(\cdot|q)\right.\right)+\sum_{\tilde{y}\in\mathcal{Y}}P(\tilde{y}|\tilde{x},\tilde{s})h\left(\tilde{f}(\tilde{s},\tilde{x},\tilde{y}),\phi(q,\tilde{y})\right) \\
&= \begin{cases} D\left(\left[\bar{p},p\right]\left\| \left[a,\bar{a}\right]\right.\right)+\bar{p}\cdot h((0,0),1)+p\cdot h((0,0),2), & \text{if } \tilde{x}=0 \\ D\left(\left[\bar{p},p\right]\left\| \left[a,\bar{a}\right]\right.\right)+\bar{p}\cdot h((0,1),1)+p\cdot h((0,1),2), & \text{if } \tilde{x}=1. \end{cases} \tag{30}
\end{aligned}$$

Under the constraints given in (17), it can be verified that  $\tilde{x} = 0$  attains the maximum in (30). Further, the left-hand side of the Bellman equation is  $\rho^* + h((0, 0), 1)$ , which, after being simplified, is exactly equal to the right-hand side of the Bellman equation. Hence, the Bellman equation holds for the case that  $(\tilde{s} = (0, 0), q = 1)$ . The verification for the remaining MDP states is omitted here and follows similar calculations.  $\square$

## APPENDIX C

### DEC — PROOF OF THEOREM 13

*Proof.* Here we provide the proof of Theorem 13 regarding the upper bound on the capacity of the DEC. As before, we start with the formulation of the channel with delayed feedback of two time instances as a new unifilar FSC with instantaneous feedback. The channel state is defined as  $\tilde{s}_{t-1} \triangleq (x_{t-2}, x_{t-1})$ , the channel input is  $\tilde{x}_t = x_t$ , and the channel output is  $\tilde{y}_t = y_{t-1}$ . The output of the DEC is  $\tilde{y}_t = x_{t-1} - x_{t-2}$  with probability  $1 - p$ , or  $\tilde{y}_t = ?$  with probability  $p$ , where  $p \in [0, 1]$  is the channel parameter.

Also here, for a particular graph-based test distribution, we solve the MDP problem of the dual capacity upper bound. Specifically, consider the following  $Q$ -graph:

$$\begin{aligned}\underline{\phi}(\underline{q}, \tilde{y} = -1) &= [1, 1, 1, 1, 1, 1, 1, 1] \\ \underline{\phi}(\underline{q}, \tilde{y} = 0) &= [1, 3, 3, 4, 4, 6, 8, 8] \\ \underline{\phi}(\underline{q}, \tilde{y} = 1) &= [6, 6, 6, 6, 6, 6, 6, 6] \\ \phi(q, \tilde{y} = ?) &= [2, 7, 7, 7, 7, 5, 7, 7].\end{aligned}\tag{31}$$

For  $a, \gamma_1, \gamma_2 \in (0, 0.5)$  and the  $Q$ -graph in (31), consider the graph-based test distribution  $T_{Y|Q}(y|q)$  that is defined by the following table:

	$q = 1$	$q = 2$	$q = 3$	$q = 4$	$q = 5$	$q = 6$	$q = 7$	$q = 8$
$y = -1$	0	$\gamma_2/2$	$a/2$	$a/2$	$\gamma_2/2$	$0.5 - \gamma_1$	$\gamma_2/2$	$a/2$
$y = 0$	$\gamma_1$	$0.5 - \gamma_2$	$0.5 - a$	$0.5 - a$	$0.5 - \gamma_2$	$\gamma_1$	$0.5 - \gamma_2$	$0.5 - a$
$y = 1$	$0.5 - \gamma_1$	$\gamma_2/2$	$a/2$	$a/2$	$\gamma_2/2$	0	$\gamma_2/2$	$a/2$
$y = ?$	0.5	0.5	0.5	0.5	0.5	0.5	0.5	0.5

The proposed graph-based test distribution follows by first numerically optimizing over the test distribution. Then, we observed that the optimal test distribution can be represented by three parameters, which are denoted here as  $\gamma_1, \gamma_2$ , and  $a$ .

Define the constant

$$\rho^* = \frac{1}{4} \log_2 \left( \frac{2 - 3a}{(1 - 2a) \cdot (1 + 8a^2\bar{a} - 3a - (1 - 4a\bar{a})\sqrt{1 + 4a^3})} \right). \quad (32)$$

Also, define  $h(\tilde{s}, q)$  as follows:

$$\begin{aligned} h((0, 0), 1) &= h((0, 0), 6) = \frac{1}{4} \log_2 \left( \frac{a(1 - 2a)\gamma_2}{4(1 - 2\gamma_2)\gamma_1^2} \right) \\ h((0, 0), 2) &= h((0, 0), 5) = h((0, 0), 7) = \frac{1}{4} \log_2 \left( \frac{4a\gamma_1^2\gamma_2}{(1 - 2a)(1 - 2\gamma_2)^3} \right) \\ h((0, 0), 3) &= h((0, 0), 4) = h((0, 0), 8) = \frac{1}{4} \log_2 \left( \frac{4a\gamma_1^2\gamma_2}{(1 - 2a)^3(1 - 2\gamma_2)} \right) \\ h((0, 1), 1) &= \frac{1}{4} \log_2 \left( \frac{a(1 - 2a^2)}{(1 - 2\gamma_1)^3} \right) \\ h((0, 1), 2) &= h((0, 1), 5) = h((0, 1), 7) = \frac{1}{4} \log_2 \left( \frac{a(1 - 2a)^2}{\gamma_2^2(1 - 2\gamma_1)} \right) \\ h((0, 1), 3) &= h((0, 1), 4) = h((0, 1), 8) = \frac{1}{4} \log_2 \left( \frac{(1 - 2a)^2}{a(1 - 2\gamma_1)} \right) \\ h((0, 1), 6) &= \frac{1}{4} \log_2 \left( \frac{a(1 - 2a)^2}{1 - 2\gamma_1} \right) \\ h((1, 0), 1) &= \frac{1}{4} \log_2 \left( \frac{a\gamma_2(1 - 2a)}{1 - 2\gamma_2} \right) \\ h((1, 0), 2) &= h((1, 0), 5) = h((1, 0), 7) = \frac{1}{4} \log_2 \left( \frac{a(1 - 2a)}{\gamma_2(1 - 2\gamma_2)} \right) \\ h((1, 0), 3) &= h((1, 0), 4) = h((1, 0), 8) = \frac{1}{4} \log_2 \left( \frac{a(1 - 2\gamma_2)}{\gamma_2(1 - 2a)} \right) \\ h((1, 0), 6) &= \frac{1}{4} \log_2 \left( \frac{a\gamma_2(1 - 2a)}{(1 - 2\gamma_1)^2(1 - 2\gamma_2)} \right) \\ h((1, 1), 1) &= \log_2 \left( \frac{1 - 2a}{2\gamma_1} \right) \\ h((1, 1), 2) &= h((1, 1), 5) = h((1, 1), 7) = \frac{1}{2} \log_2 \left( \frac{1 - 2a}{1 - 2\gamma_2} \right) \\ h((1, 1), 3) &= h((1, 1), 4) = h((1, 1), 8) = 0 \\ h((1, 1), 6) &= \frac{1}{4} \log_2 \left( \frac{a(1 - 2a)^2}{4\gamma_1^2(1 - 2\gamma_1)} \right). \end{aligned} \quad (33)$$

Let us assume that the optimal policy is given by

$$u^*(\tilde{s}, q) = \begin{cases} 1, & (\tilde{s} = (1, 1), q = 1), \\ 0, & \text{else.} \end{cases} \quad (34)$$

The policy above was obtained by solving numerically the MDP problem using the value iteration algorithm. Assuming (34), it can be noted that the Bellman equation is based on a finite set of linear equations, and it can be verified that if

$$\begin{aligned}\gamma_1 &= \frac{1}{4a} \left( (2 - 4a) \cdot \sqrt{a^2 + 0.25} + 4a\bar{a} - 1 \right) \\ \gamma_2 &= \frac{1}{4 - 6a} \left( (4a^2 - 4a + 1)\sqrt{1 + 4a^2} - 8a^2\bar{a} + 1 \right),\end{aligned}\quad (35)$$

then the Bellman equation holds under our choice of  $\rho^*$  in (32) and the function  $h(\tilde{s}, q)$  in (33). The verification follows from straightforward calculations, as we did in the previous sections, and therefore the details are omitted here. In Eq. (35), we write analytical expressions for  $\gamma_1, \gamma_2$  as a function of  $a$ . These expressions were derived by observing that, for particular MDP states, the optimal solution (in terms of the test distribution's parameters) is achieved when the right-hand side of the Bellman equation does not depend on the action. Namely, for particular MDP states we require that the right-hand side of the Bellman equation is equal for  $u = 0$  and  $u = 1$ . Such a requirement results in linear equality constraints that are satisfied with  $\gamma_1$  and  $\gamma_2$  in (35).  $\square$

## REFERENCES

- [1] B. Huleihel, O. Sabag, and H. H. Permuter, "Capacity of the trapdoor channel with delayed feedback," in *Proc. IEEE Int. Symp. Inf. Theory (ISIT)*, 2022, pp. 492–497.
- [2] B. McMillan, "The basic theorems of information theory," *Ann. Math. Statist.*, vol. 24, no. 2, pp. 196–219, Jun. 1953.
- [3] C. E. Shannon, "Certain results in coding theory for noisy channels," *Inf. Control*, vol. 1, pp. 6–25, Sep. 1957.
- [4] D. Blackwell, L. Breiman, and A. Thomasian, "Proof of Shannon's transmission theorem for finite-state indecomposable channels," *Ann. Math. Stat.*, vol. 29, pp. 1209–1220, 1958.
- [5] P. Sadegh, R. A. Kennedy, P. B. Rapajic, and R. Shams, "Finite-state Markov modeling of fading channels - a survey of principles and applications," *IEEE Signal Process. Mag.*, vol. 25, no. 5, pp. 57–80, Sep. 2008.
- [6] Q. Zhang and S. A. Kassam, "Finite-state Markov model for Rayleigh fading channels," *IEEE Trans. Commun.*, vol. 47, no. 11, pp. 1688–1692, Nov. 1999.
- [7] H. S. Wang and N. Moayeri, "Finite-state markov channel-a useful model for radio communication channels," *IEEE Trans. Inf. Theory*, vol. 44, pp. 163–171, 1995.
- [8] L. Galluccio, A. Lombardo, G. Morabito, S. Palazzo, C. Panarello, and G. Schembra, "Capacity of a binary droplet-based microfluidic channel with memory and anticipation for flow-induced molecular communications," *IEEE Transactions on Communications*, vol. 66, no. 1, pp. 194–208, Jan. 2018.
- [9] N. Farsad, H. B. Yilmaz, A. Eckford, C. Chae, and W. Guo, "A comprehensive survey of recent advancements in molecular communication," *IEEE Communications Surveys Tutorials*, vol. 18, no. 3, pp. 1887–1919, thirdquarter 2016.
- [10] K. A. S. Immink, P. H. Siegel, and J. K. Wolf, "Codes for digital recorders," *IEEE Trans. Inf. Theory*, vol. 44, no. 6, pp. 2260–2299, Oct. 1998.
- [11] J. Chen and T. Berger, "The capacity of finite-state Markov channels with feedback," *IEEE Trans. Inf. Theory*, vol. 51, pp. 780–789, Mar. 2005.
- [12] H. H. Permuter, P. Cuff, B. V. Roy, and T. Weissman, "Capacity of the trapdoor channel with feedback," *IEEE Trans. Inf. Theory*, vol. 54, no. 7, pp. 3150–3165, Jul. 2008.
- [13] O. Elishco and H. Permuter, "Capacity and coding for the Ising channel with feedback," *IEEE Trans. Inf. Theory*, vol. 60, no. 9, pp. 5138–5149, Sep. 2014.
- [14] O. Sabag, H. Permuter, and N. Kashyap, "The feedback capacity of the binary erasure channel with a no-consecutive-ones input constraint," *IEEE Trans. Inf. Theory*, vol. 62, no. 1, pp. 8–22, Jan. 2016.
- [15] J. Wu and A. Anastasopoulos, "On the capacity of the chemical channel with feedback," in *Proc. of IEEE Int. Symp. Inf. Theory (ISIT)*, Jul. 2016, pp. 295–299.
- [16] A. Sharov and R. M. Roth, "On the capacity of generalized Ising channels," *IEEE Trans. Inf. Theory*, vol. 63, no. 4, pp. 2338–2356, Apr. 2017.
- [17] E. Shmuel, O. Sabag, and H. H. Permuter, "The feedback capacity of noisy output is the STate (NOST) channels," *IEEE Trans. Inf. Theory*, vol. 68, no. 8, pp. 5044–5059, Apr. 2022.
- [18] O. Peled, O. Sabag, and H. H. Permuter, "Feedback capacity and coding for the  $(0, k)$  -RLL input-constrained BEC," *IEEE Trans. Inf. Theory*, vol. 65, no. 7, pp. 4097–4114, Jul. 2019.
- [19] O. Sabag, H. H. Permuter, and N. Kashyap, "Feedback capacity and coding for the BIBO channel with a no-repeated-ones input constraint," *IEEE Trans. Inf. Theory*, vol. 64, no. 7, pp. 4940–4961, Jul. 2018.
- [20] Z. Aharoni, O. Sabag, and H. H. Permuter, "Feedback capacity of Ising channels with large alphabet via reinforcement learning," *IEEE Trans. Inf. Theory*, vol. 68, no. 9, pp. 5637–5656, Apr. 2022.

- [21] O. Sabag, H. H. Permuter, and H. D. Pfister, "A single-letter upper bound on the feedback capacity of unifilar finite-state channels," *IEEE Trans. Inf. Theory*, vol. 63, no. 3, pp. 1392–1409, Mar. 2017.
- [22] O. Sabag, B. Huleihel, and H. H. Permuter, "Graph-based encoders and their performance for finite-state channels with feedback," *IEEE Trans. Commun.*, vol. 68, no. 4, pp. 2106–2117, Apr. 2020.
- [23] O. Sabag and H. H. Permuter, "The duality upper bound for unifilar finite-state channels with feedback," in *International Zurich Seminar on Information and Communication (IZS)*, Feb. 2020, pp. 68–72.
- [24] R. Ahlswede and A. Kaspi, "Optimal coding strategies for certain permuting channels," *IEEE Trans. Inf. Theory*, vol. 33, no. 3, pp. 310–314, May 1987.
- [25] R. Ahlswede, N. Cai, and Z. Zhang, "Zero-error capacity for models with memory and the enlightened dictator channel," *IEEE Trans. Inf. Theory*, vol. 44, no. 3, pp. 1250–1252, May 1998.
- [26] K. Kobayashi, H. Morita, and M. Hoshi, "Some considerations on the Trapdoor channel," in *Proc. of 3rd Asian-European Workshop on Inf. Theory*, 2003, pp. 9–10.
- [27] T. Lutz, "Recursions for the trapdoor channel and an upper bound on its capacity," in *Proc. IEEE Int. Symp. Inf. Theory (ISIT)*, Jun. 2014, pp. 2914–2918.
- [28] B. Huleihel, O. Sabag, H. H. Permuter, N. Kashyap, and S. Shamai, "Computable upper bounds on the capacity of finite-state channels," *IEEE Trans. Inf. Theory*, pp. 1–1, Jun. 2021.
- [29] D. Blackwell, *Information Theory. Modern mathematics for the engineer: Second series*, pp. 182–193, 1961.
- [30] G. Han and B. Marcus, "Asymptotics of entropy rate in special families of hidden Markov chains," *IEEE Trans. Inf. Theory*, vol. 56, no. 3, pp. 1287–1295, Mar. 2010.
- [31] A. Thangaraj, "Dual capacity upper bounds for noisy runlength constrained channels," *IEEE Trans. Inf. Theory*, vol. 63, no. 11, pp. 7052–7065, Nov. 2017.
- [32] E. Zehavi and J. Wolf, "On runlength codes," *IEEE Trans. Inf. Theory*, vol. 34, no. 1, pp. 45–54, Jan. 1988.
- [33] G. Han and B. Marcus, "Concavity of the mutual information rate for input-restricted memoryless channels at high SNR," *IEEE Trans. Inf. Theory*, vol. 58, no. 3, pp. 1534–1548, Mar. 2012.
- [34] H. D. Pfister and P. H. Siegel, "Joint iterative decoding of LDPC codes for channels with memory and erasure noise," *IEEE Journal on Selected Areas in Communications*, vol. 26, no. 2, pp. 320–337, Feb. 2008.
- [35] H. D. Pfister, "On the capacity of finite state channels and the analysis of convolutional accumulate- $m$  codes," Ph.D. dissertation, University of California, San Diego, La Jolla, 2003.
- [36] H. H. Permuter, T. Weissman, and A. J. Goldsmith, "Finite state channels with time-invariant deterministic feedback," *IEEE Trans. Inf. Theory*, vol. 55, no. 2, pp. 644–662, Feb. 2009.
- [37] A. Arapostathis, V. S. Borkar, E. Fernandez-Gaucherand, M. K. Ghosh, and S. Marcus, "Discrete time controlled Markov processes with average cost criterion - a survey," *SIAM Journal of Control and Optimization*, vol. 31, no. 2, pp. 282–344, 1993.
- [38] O. Shayevitz and M. Feder, "Optimal feedback communication via posterior matching," *IEEE Trans. Inf. Theory*, vol. 57, no. 3, pp. 1186–1222, Mar. 2011.
- [39] O. Sabag, B. Huleihel, and H. H. Permuter, "Implementation of graph-based encoders and their performance for finite-state channels with feedback," 2019, [Online]. Available: <https://github.com/Basharh1/Graph-Based-Encoders-and-their-Performance-for-Finite-State-Channels-with-Feedback>.
- [40] F. Topsøe, "An information theoretical identity and a problem involving capacity," *Studia Scientiarum Mathematicarum Hungarica*, vol. 2, pp. 291–292, 1967.
- [41] S. Yang, A. Kavčić, and S. Tatikonda, "Feedback capacity of finite-state machine channels," *IEEE Trans. Inf. Theory*, vol. 51, no. 3, pp. 799–810, Mar. 2005.
- [42] O. Sabag, V. Kostina, and B. Hassibi, "Feedback capacity of Gaussian channels with memory," in *Proc. IEEE Int. Symp. Inf. Theory (ISIT)*, 2022, pp. 2547–2552.
- [43] T. Berger, "The generalized Shannon-Blackwell billiard ball channel," in *Lecture 2 of CSL, University of Illinois, Urbana, IL ("Information Theory Invades Biology")*, 22 Apr. 2002.
- [44] R. Ash, *Information Theory*. New York: Wiley, 1965.
- [45] C. Shannon, "The zero error capacity of a noisy channel," *IEEE Trans. Inf. Theory*, vol. 2, no. 3, pp. 8–19, Sep. 1956.
- [46] P. Vontobel, A. Kavcic, D. Arnold, and H.-A. Loeliger, "A generalization of the Blahut-Arimoto algorithm to finite-state channels," *IEEE Trans. Inf. Theory*, vol. 54, no. 5, pp. 1887–1918, May 2008.
- [47] Y. Li and G. Han, "Input-constrained erasure channels: Mutual information and capacity," in *Proc. IEEE Int. Symp. Inf. Theory (ISIT)*, Jun. 2014, pp. 3072–3076.
- [48] D. M. Arnold, H.-A. Loeliger, P. O. Vontobel, A. Kavčić, and W. Zeng, "Simulation-based computation of information rates for channels with memory," *IEEE Trans. Inf. Theory*, vol. 52, no. 8, pp. 3498–3508, Aug. 2006.
- [49] H. D. Pfister, "The capacity of finite state channels," Ph.D. dissertation Chapter 4, 2003.